

1 **Dynamic and Thermodynamic Processes Related to Sea-Ice Surface**
2 **Melt Advance in the Laptev Sea and East Siberian Sea**

3
4 Hongjie LIANG,¹ Wen ZHOU^{1,2}

5 ¹ *Department of Atmospheric and Oceanic Sciences & Institute of Atmospheric Sciences, Fudan*
6 *University, Shanghai, China*

7 ² *Center for Polar Ice & Snow and Climate Change Research, Polar Research Institute of China,*
8 *Shanghai, China*

9
10
11 *Correspondence to: Wen Zhou (wen_zhou@fudan.edu.cn)*

12
13
14
15 *Aug, 2023*
16

17 ABSTRACT

18 Arctic summer sea ice has shrunk considerably in recent decades. This study
19 investigates springtime sea-ice surface melt onset ~~in springtime~~ in the Laptev Sea and
20 East Siberian Sea, which are key seas along the Northeast Passage. ~~Instead of region-~~
21 ~~mean melt onset, we define an index of~~ Melt Advance, which is ~~defined as~~ the areal
22 percentage of a sea that has experienced sea-ice surface melting before the end of May;
23 ~~is used instead of region mean melt onset.~~ Four representative scenarios of Melt
24 Advance in the region are identified. Each scenario is ~~accompanied driven~~ by a
25 ~~combination of~~ distinct patterns between atmospheric circulation, atmospheric
26 thermodynamic state, sea ice cover (polynya activity), and surface energy balance in
27 May, in the lower troposphere in May, which regulates sea ice dynamics and air mass
28 ~~transport, further influencing surface energy balance and Melt Advance.~~ In general,
29 concurrent with faster Melt Advance are warmer and wetter atmosphere, ~~reduced less~~
30 sea ice cover, and surface energy gains in spring. Melt Advance, ~~as well as like~~ sea ice
31 cover in May, is significantly correlated with summer sea ice cover. This study
32 implicates the interannual and interdecadal flexibility of spring circulation in the lower
33 troposphere and the significance of seasonal evolution in the Arctic.

34
35
36 **1. Introduction**

37 Since the 1970s, satellites have enabled global detection of the Earth. Arctic
38 summer sea ice extent is found to have decreased dramatically in the past four decades
39 (Petty et al., 2020; Stroeve and Notz, 2018), which is a prominent indicator of global
40 warming. In fact, the Arctic has a faster warming trend than elsewhere on the planet,
41 especially in the lower troposphere during the cold season (Cohen et al., 2014; Serreze
42 et al., 2009; Screen and Simmonds, 2010). This phenomenon, called Arctic
43 Amplification, presumably results from reduced sea ice cover and enhanced oceanic
44 energy release toward the atmosphere, atmospheric and oceanic heat transport from

45 lower latitudes, and local positive feedbacks (Serreze et al., 2009; Cohen et al., 2014;
46 Taylor et al., 2022). Some research has indicated that the mid-latitudes may frequently
47 experience severe winters due to the Arctic Amplification which reduces the meridional
48 temperature gradient and in turn amplifies the planetary Rossby wave and makes it
49 more stationary (Francis and Vavrus, 2015). In the Arctic, positive ice-albedo feedback
50 is active in the melt season (Budyko, 1969; Kashiwase et al., 2017; Sellers, 1969): after
51 sea ice begins to melt in spring, surface albedo decreases substantially, which favors
52 more solar radiation absorption and promotes further sea ice melting. Based on this
53 notion, some studies have tried to predict Arctic summer sea ice cover by sea-ice surface
54 Melt Onset (MO) in spring, i.e., the date when the sea ice surface begins to form liquid
55 water (Petty et al., 2017; Wang et al., 2011). Currently, satellite remote sensing helps
56 us construct the pan-Arctic sea ice MO, which is not possible with only in-situ field
57 observations. ~~For~~ However, for sea ice lateral and bottom melting, satellites are less
58 useful and buoys are widely employed (Lei et al., 2022).

59 Many studies have touched on sea ice MO in springtime (Drobot and Anderson,
60 2001; Bliss and Anderson, 2014; Horvath et al., 2021; Crawford et al., 2018; Markus et
61 al., 2009; Stroeve et al., 2014). Generally, sea ice MO is becoming earlier in most parts
62 of the Arctic, which is consistent with the Arctic warming ~~trend~~. Another notable feature
63 of MO is its regionality. For example, the Barents Sea, Kara Sea, Laptev Sea, and East
64 Siberian Sea are around the same latitudes along the Siberian coast, but the MO trends
65 were -7.1, -5.2, -2.8, and -1.8 days per decade from 1979 to 2013, respectively (Stroeve
66 et al., 2014). Liang and Su (2021) investigated the interannual early/late relationship of
67 MO between the Laptev Sea and East Siberian Sea, which is related to the large-scale
68 atmospheric pattern of the Barents Oscillation (Skeie, 2000). Locally, synoptic
69 processes are regarded as responsible for interannual variability. Mortin et al. (2016)
70 argued that sea ice MO is generally associated with higher surface air temperature
71 (SAT), total-column water vapor (TWV), and cloud cover, which promotes downward
72 longwave radiation.

73 The Laptev Sea (LS) and East Siberian Sea (ESS) are marginal seas of the Arctic
74 Ocean, north of Siberia along the Northeast Passage (Fig. S1). The longitude-latitude
75 ranges are around 70°N-80°N and 100°E-180°, covering 0.66 and 1.14 million km² for
76 the LS and ESS, respectively. These two seas are among the regions where sea ice
77 decline in September during the past four decades has been the most prominent, and
78 they are key regions for safe transportation across the Northeast Passage. In spring, sea
79 ice almost completely covers the seas, while in summer, sea ice substantially retreats
80 off the coast.

81 Focusing on the Laptev SeaLS and East Siberian SeaESS, which usually have the
82 heaviest ice blockmost persistent sea ice coverage in the Northeast Passage, this study
83 aims to demonstrate the springtime processes related to different MO-Melt Advance
84 scenarios and explore the linkage between springtime MO-Melt Advance and
85 summertime sea ice coverage.

86

87

88 **2. Data and Methods**

89 Sea ice Melt Onset (MO) is the date when the sea ice surface begins to melt in
90 spring, which is retrieved from satellite passive microwave signals (Markus et al., 2009).
91 Liquid water has greater emissivity than ice/snow, so surface melting invokes changes
92 in passive microwave signals. The dataset is distributed by the National Aeronautics
93 and Space Administration (NASA) Cryospheric Sciences Research Portal. We use the
94 yearly MO from 1979 to 2018, with a spatial resolution of ~25 km. Following the
95 method in Liang and Su (2021), we fill in the missing MO values based on surface air
96 temperature (SAT) datasets from the International Arctic Buoy Programme/Polar
97 Exchange at the Sea Surface (IABP/POLES) for 1979-2004 and the Atmospheric
98 InfraRed Sounder (AIRS) for 2005-2018. Although the missing values are not quite a
99 lot, the analysis here is more convenient if the whole research area in the LS and ESS
100 is covered.

101 The sea ice concentration (SIC) dataset, called Ocean and Sea Ice Satellite
102 Application Facility (OSI SAF), is from the European ~~Organisation~~ Organization for the
103 Exploitation of Meteorological Satellites (EUMETSAT) (Lavergne et al., 2019). We
104 use the monthly SIC in May from 1979 to 2018, with a resolution of 25 km. We also
105 examine SIC dataset by the NASA Team algorithm(Cavalieri et al., 1996), which shows
106 basically the same patterns in May as OSI SAF.

107 The atmospheric variables and surface energy fluxes are from the ERA5 reanalysis
108 by the European Centre for Medium-Range Weather Forecasts (ECMWF) (Hersbach et
109 al., 2020), which replaces the ERA-Interim reanalysis that ceased production in 2019.
110 The variables used in this study are monthly downward longwave radiation (DLR), net
111 longwave radiation (NLR), downward shortwave radiation (DSR), net shortwave
112 radiation (NSR), surface latent heat flux (SLHF), surface sensible heat flux (SSHF),
113 total-column water vapor (TWV), and SAT and wind fields at the 850-hPa level, for the
114 month of May from 1979 to 2018. The spatial resolution of ERA5 used in this study is
115 $0.25^{\circ} \times 0.25^{\circ}$, less than 30 km in the region of the Laptev Sea and East Siberian Sea.
116 Note that the four components of the surface energy balance (SEB) include longwave
117 radiation~~NLR~~, shortwave radiation~~NSR~~, surface latent heat flux (SLHF), and surface
118 sensible heat flux (SSHF).

119

120

121 3. Results

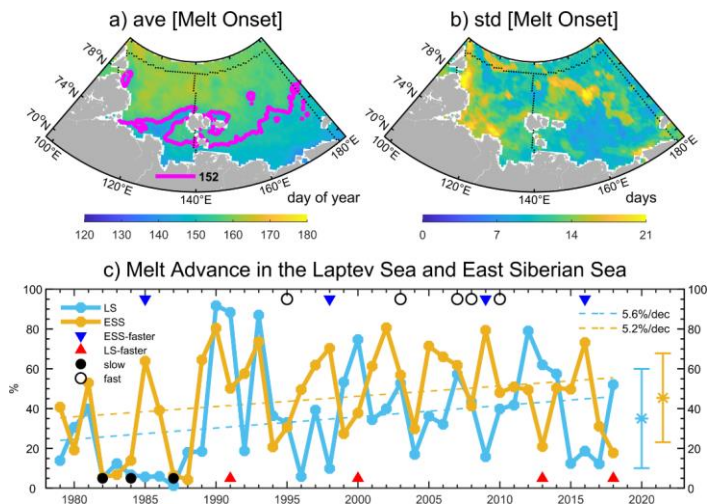
122 3.1 Distinct Melt Advance Scenarios in the Laptev Sea and East Siberian Sea

123 ~~The Laptev Sea (LS) and East Siberian Sea (ESS) are marginal seas of the Arctic~~
124 ~~Ocean, north of Siberia along the Northeast Passage (Fig. S1). The longitude-latitude~~
125 ~~ranges are around 70°N–80°N and 100°E–180°, covering 0.66 and 1.14 million km² for~~
126 ~~the LS and ESS, respectively. These two seas are among the regions where sea-ice~~
127 ~~decline in September during the past four decades has been the most prominent, and~~
128 ~~they are key regions for safe transportation across the Northeast Passage. Meanwhile,~~

129 ~~sea ice surface Melt Onset (MO) in spring generally tends to be earlier. In spring, sea~~
130 ~~ice almost completely covers these two seas, while in summer, sea ice substantially~~
131 ~~retreats off the coast.~~ Sea ice ~~first~~ begins to melt at the surface in spring when solar
132 radiation increases and the atmosphere warms. On average, the sea ice surface in the
133 Laptev Sea (LS) and East Siberian Sea (ESS) begins to melt during May and June (Fig.
134 1a). Naturally, sea ice melting advances northward in a given year. The range for the
135 ~~interannually change of,~~ MO in a given place is expected to ~~change within~~ be around
136 one month (Fig. 1b). In order to demonstrate the progress of MO in different years, melt
137 advance (MA) is defined by calculating the areal percentage of an individual sea that
138 has experienced MO at the end of May (see magenta contour line in Fig. 1a). In this
139 way, we can detect whether sea-ice surface melting advances slowly or quickly in a
140 specific year, as well as the spatial patterns of the melt advance. For the seasonal
141 prediction of summer sea ice, this metric of Melt Advance is in essence similar to the
142 average MO date, but may have advantages if we can get real-time satellite MO for the
143 region. Then, at the end of May or other specific date, we can get the MA pattern which
144 supports timely seasonal prediction. ~~is date-dependent and useful, unlike the region-~~
145 ~~mean MO, which necessitates waiting for complete melting throughout the whole sea.~~

146 Figure 1c shows the time series of MA for the LS and ESS during 1979-2018. The
147 variability is large, ranging from near zero to 100%. This implies changeable spring
148 conditions on the interannual scale. On average, MA is around 40% for each sea,
149 meaning that ~40% of the sea area has experienced sea-ice surface melting at the end
150 of May. In the context of global warming, MA has an increasing tendency in both seas
151 although this tendency is not quite significant (less than 6% per decade). This indicates
152 that we sometimes need to pay more attention to the interannual variability than to the
153 long-term linear tendency. We can also notice that relatively slow MA in the 1980s
154 contributes considerably to the overall positive tendency.

155



156
 157 **Fig. 1.** (a, b) Climatology and standard deviation of sea ice Melt Onset, and (c) Melt
 158 Advance time series in the Laptev Sea and East Siberian Sea, 1979-2018. The magenta
 159 lines in panel (a) are contours of 152 (day of year), representing the end of May. The
 160 areal percentage of sea ice Melt Onset earlier than 152 (day of year) is defined as Melt
 161 Advance. In panel (c), only the trend of Melt Advance in the ESS is statistically
 162 significant at the 90% confidence level. The average and standard deviation of the Melt
 163 Advance in the LS and ESS are $35\% \pm 25\%$ and $45\% \pm 22\%$, respectively. Sample years
 164 (16 out of the long time-series) that fall into one of Four-four categories of sample years
 165 are marked (see also Table 1).

166

167 Another feature is related to the relationship of MA between the LS and ESS. In
 168 some years, MA in both the LS and ESS is slow, as in the 1980s; in other years, MA in
 169 both seas may be fast; and in other years, MA can be substantially different in the two
 170 seas. Thus, four categories of sample years are selected for further composite analysis
 171 (Table 1 and markers in Fig. 1c; MA difference between the LS and ESS is shown in
 172 Fig. S2), which represent four basic scenarios of MA in this region. Specifically, years
 173 with significantly faster MA in the ESS than in the LS ($\delta > 48\%$) are grouped as the ESS-
 174 faster-scenario, while years with significantly faster MA in the LS than in the ESS
 175 ($\delta > 33\%$) are classified as the LS-faster-scenario. The slow-scenario includes years
 176 when MA in both seas is slow (below 20%), while the fast-scenario consists of years
 177 when MA in both seas is relatively fast (between 30% and 60% at the same time). So,

178 two pairs of contrasting categories are formed (ESS-faster-scenario vs. LS-faster-
 179 scenario, slow-scenario vs. fast-scenario). Note that to some extent the latter two
 180 scenarios represent the contrast between the 1980s and subsequent decades. Such
 181 categorization also reflects the large variability of MA in spring from the interannual
 182 perspective.

183

Category	Years	Description
ESS-faster-scenario	1985, 1998, 2009, 2016	significantly faster Melt Advance ($\delta > 48\%$) in the ESS than in the LS
LS-faster-scenario	1991, 2000, 2013, 2018	significantly faster Melt Advance ($\delta > 33\%$) in the LS than in the ESS
slow-scenario	1982, 1984, 1987	similar but slow Melt Advance ($\delta < 8\%$, but below 20%)
fast-scenario	1995, 2003, 2007, 2008, 2010	similar but fast Melt Advance ($\delta < 9\%$, but between 30% and 60%)

184 **Table 1** List of years under different scenarios of Melt Advance.

185 Note: Practically, the ESS-faster-scenario and LS-faster-scenario are selected based on
 186 one standard deviation of the difference in Melt Advance between the Laptev Sea and
 187 East Siberian Sea. The slow-scenario and fast-scenario include years when Melt
 188 Advance in the two seas is quite close. All years listed here are marked in Fig. 1c.

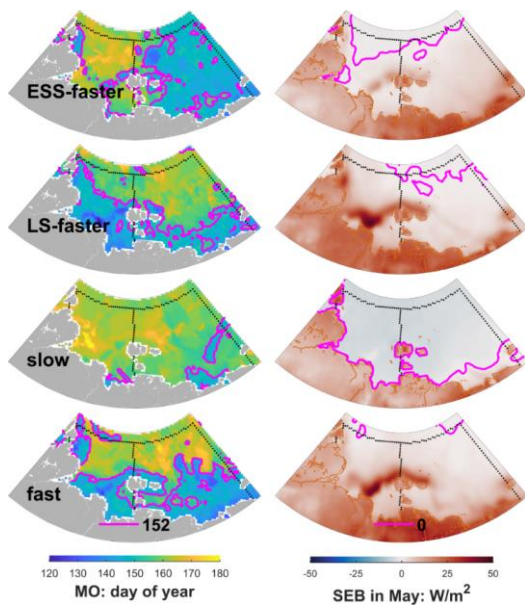
189

190 Composite results show that the ESS-faster-scenario has substantially earlier MO,
 191 i.e., faster MA in the ESS than in the LS, while the LS-faster-scenario has a somewhat
 192 opposite signal (indicated by the magenta line in Fig. 2). For the slow-scenario, little
 193 area in either sea has experienced MO until the end of May, indicating slow MA; for
 194 the fast-scenario, nearly half of both seas has begun to experience sea-ice surface
 195 melting, indicating fast MA at almost the same pace. From the surface energy balance
 196 (SEB) in May, we find consistent patterns. With the zero lines of SEB as a reference,
 197 the ESS-faster-scenario has relatively more positive SEB in the ESS than in the LS,
 198 while the opposite is true for the LS-faster-scenario. For the slow-scenario, SEB is
 199 negative over most of the two seas, while for the fast-scenario, SEB is positive in both
 200 seas. This fits well with common sense. Although MA-related albedo changes may
 201 amplify the SEB signals in a two-way interaction, it is fair to say that SEB in May

202 drives different patterns of MA (see individual years in Fig. S3).

203 In the next section, we investigate systematic processes under different MA
204 scenarios that involve the atmosphere, sea ice, and surface energy fluxes. ~~Note that the~~
205 ~~four components of SEB include longwave radiation, shortwave radiation, surface~~
206 ~~latent heat flux (SLHF), and surface sensible heat flux (SSHF).~~

207



208

209 **Fig. 2.** Composites of MO and surface energy balance (SEB) in May for the four
210 scenarios. The left column shows the MO patterns marked by magenta contour lines
211 with the value of 152 (day of year) which represents the end of May. The right column
212 is the SEB in May, with magenta contour lines of zero. Black dots denote the boundaries
213 of the LS and ESS.

214

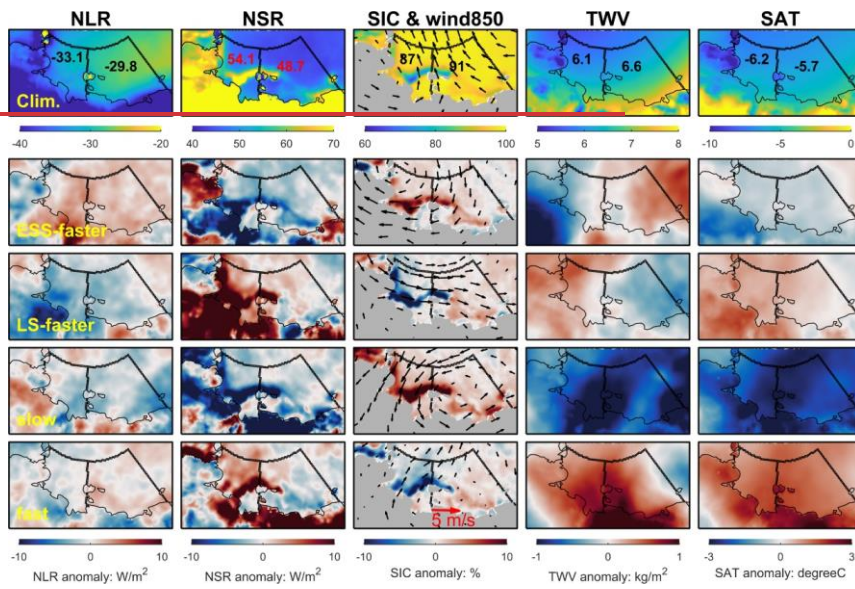
215

216 3.2 Dynamic and Thermodynamic Processes under Different Melt Advance Scenarios

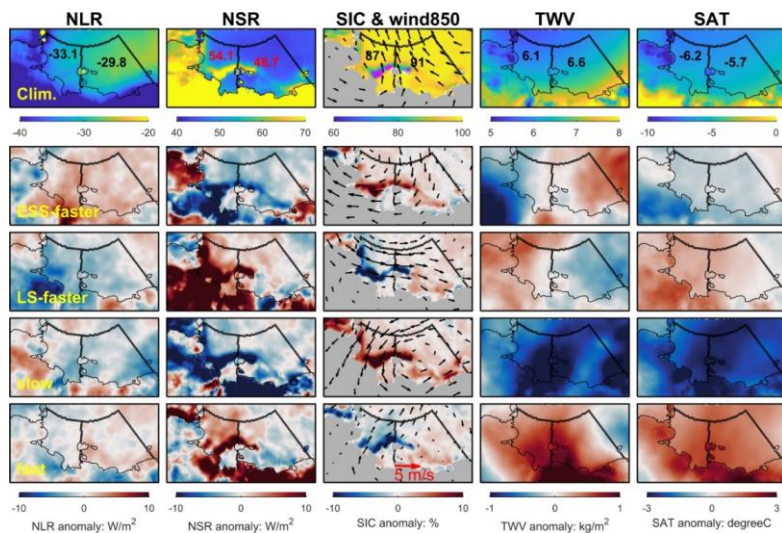
217 Climatologically, SEB is basically positive ($\sim 5 \text{ W/m}^2$) across the two seas in May
218 (see first row in Fig. S4). Among the components, it is positive net shortwave radiation
219 (NSR) that compensates for losses from net longwave radiation (NLR), SLHF, and
220 SSHF. This implies that on average the atmosphere receives energy from the surface

221 through the latter three components in May. SAT is around -6°C , while sea ice almost
 222 fully covers the ocean ($\sim 90\%$) (see first row in Fig. 3). In the lower troposphere (850
 223 hPa), southeasterlies blow across the region, which to some extent explains the
 224 existence of polynyas in the middle LS, i.e., regions where sea ice concentration is
 225 below 75%. Note that Fig. 3 shows only selected vital variables; other relevant factors
 226 can be found in Fig. S4-S7.

227



228



229

230 **Fig. 3.** Climatology (first row) and composite anomalies for the four scenarios (lower
 231 four rows) of relevant atmospheric and sea ice variables in May: NLR, NSR, SIC, winds
 232 at 850 hPa, TWV, and SAT. Numbers within the LS and ESS are the region-mean values,
 233 respectively. Note that magenta lines in the climatological SIC fields denote contours
 234 of 75% SIC values, which suggest the location of polynyas.

235

236 In the ESS-faster-scenario (see second row in Fig. 3 and blue bars in Fig. 4),
 237 prevailing northeasterlies in the lower troposphere ~~push and consolidate the sea ice~~
 238 ~~against the land~~ tend to increase SIC and reduce polynya area, especially for the LS,
 239 which increases surface albedo and decreases solar radiation absorption. The
 240 northeasterlies seem to also bring slightly cool air masses to the region, and slightly
 241 moist air masses to the ESS. As a whole, the atmospheric state is close to climatology
 242 as shown by small SAT and TWV anomalies. Given that sea ice cover is more packed,
 243 longwave radiation loss from the surface to the atmosphere is reduced, which to some
 244 extent compensates for the reduced solar radiation absorption. Due to the greater
 245 ~~reduction-negative anomaly~~ of solar radiation absorption in the LS, the net surface
 246 energy balance is a loss in the LS, but a gain in the ESS (Fig. S4 and S6). In addition,
 247 sea-ice surface melting is usually preconditioned by increased water vapor in the
 248 atmosphere (Mortin et al., 2016). So, faster Melt Advance in the ESS is expected as

249 TWV is increased in the ESS.

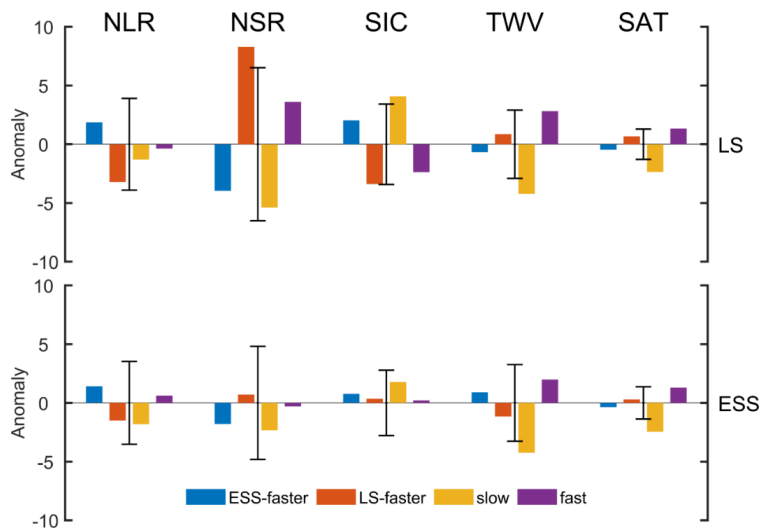
250 For the LS-faster-scenario (see third row in Fig. 3 and red bars in Fig. 4), wind fields
251 at 850-hPa show unified westerlies over the LS and northwesterlies over the ESS, which
252 to some extent account for the reduced sea ice cover in the LS and the slightly packed
253 sea ice in the ESS. Such circulation has offshore wind component in the LS and drive
254 sea ice out of the LS, which probably leads to more polynya opening and reduced SIC
255 (Krumpfen et al., 2011). So, we see a substantial increase in solar radiation absorption
256 (beyond one standard deviation) in the LS. ~~Given that~~While longwave radiation loss is
257 somehow enhanced, the net surface energy balance is still a gain for the LS and a loss
258 for the ESS. The westerlies may also bring warm and wet air masses from the North
259 Atlantic and contribute to positive anomalies of TWV and SAT in the LS, which
260 promotes faster MA. ~~It is also possible~~We may expect that reduced sea ice cover in the
261 LS enables more moisture to be released from the exposed ocean. However, latent heat
262 loss as well as sensible heat loss toward atmosphere in the LS weakens (Fig. S4 and
263 S6), which suggests that warmer and moister atmosphere is mainly a result of air mass
264 transport and in turn reduces turbulent heat loss from the surface.

Formatted: Indent: First line: 1.5 ch

265

266

267



268

269 **Fig. 4.** Region-mean composite anomalies in the LS and ESS for the four scenarios
 270 shown in Fig. 3. The error bars denote the corresponding standard deviation for 1979-
 271 2018. The variables of NLR, NSR, SIC, TWV, and SAT have units of W/m^2 , W/m^2 , %,
 272 kg/m^2 , and K, respectively. Here, SIC is represented by the areal percentage of sea ice
 273 cover relative to the whole sea. To facilitate viewing, TWV is scaled by a factor of 5.

274

275 For the slow-scenario, ~~with three sample years from the 1980s~~ (see fourth row in
 276 Fig. 3, and orange bars in Fig. 4), a cyclonic anomaly in the lower troposphere, which
 277 is centered on the ESS, pushes sea ice against the southern coast in the LS. More sea
 278 ice cover in both seas decreases solar radiation absorption. Meanwhile, ~~this circulation~~
 279 ~~also brings~~ this region is under the influence of cold and dry air masses (beyond one
 280 standard deviation), which induce a large loss of longwave radiation and SSHF from
 281 the surface. As a whole, we see unified surface energy deficits in the LS and ESS
 282 (beyond one standard deviation). ~~Slow MA is also expected for this region. Note that~~
 283 ~~all the three sample years are from the 1980s. So, the larger sea ice cover and cooler~~
 284 ~~atmosphere mainly reflect the Arctic state in the 1980s, which is a decadal phenomenon~~
 285 ~~rather than interannual characteristics. We also examine the monthly snowfall under the~~
 286 ~~four scenarios (Fig. S5). For this region, snowfall dominates the total precipitation in~~
 287 ~~May. Especially for the slow melt advance scenario, snowfall is abnormally high, which~~

288 will also result in high surface albedo.

289 For the fast-scenario, with sample years after the 1980s (see last row in Fig. 3, and
290 purple bars in Fig. 4), southerlies in the lower troposphere blow mainly across the LS,
291 which drive sea ice off the coast, open the polynya and in turn increase shortwave
292 radiation absorption. At the same time, the southerlies bring warm and wet air masses
293 to this region, which substantially reduce the SSHF loss from the surface. As a result,
294 we see a positive net surface energy balance in this region and relatively fast MA.

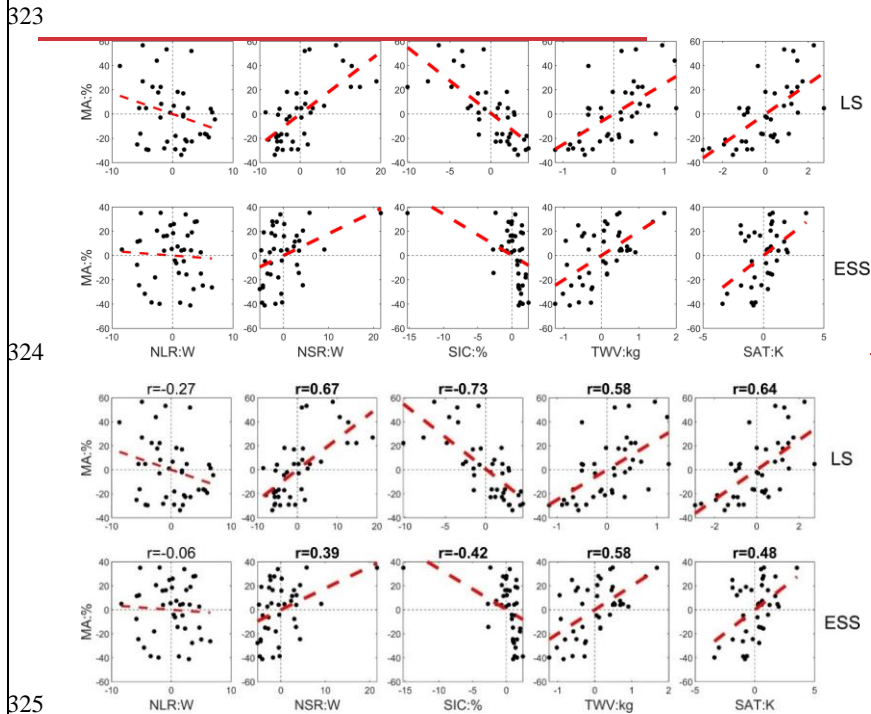
295 The composite analysis above indicates that circulation in the lower troposphere in
296 spring in this region can be quite changeable (see individual years in Fig. S8), which
297 can have two effects: one is related to sea ice dynamics; the other involves moisture
298 and ~~warm~~ air mass advection. The former produces strong regulation of NSR due to
299 albedo changes, while the latter has everything to do with the atmospheric state, which
300 favors sea-ice surface melting when the atmosphere is warm and wet.

301 Figure 5 further shows the statistical correlation related to MA, ~~incorporating~~
302 covering years from 1979 to 2018. In general, we see that faster MA is accompanied by
303 warm and wet atmosphere. The related atmospheric circulation in the lower troposphere
304 may also drive reduced SIC and subsequent increased solar radiation absorption. In
305 addition, ~~previous studies have~~ Mortin et al. (2016) argued that on a synoptic scale,
306 increased water vapor in the atmosphere favors stronger DLR, which promotes sea-ice
307 surface melting (~~Mortin et al., 2016~~). Such conclusion makes sense when we focus on
308 sea ice and atmosphere above. While we examine from the perspective of the whole
309 region, including effects of the open ocean. The results here suggests that on the
310 subseasonal scale net longwave radiation has little connection with MA (see first
311 column in Fig. 5). To some extent, the weak correlation even shows that on the monthly
312 scale, longwave radiation loss tends to be more when SEB is more and MA is faster,
313 which suggests some negative feedback probably related to the open ocean.

314 While NSR is strong, downward shortwave radiation tends to be less (see Fig. S9),
315 which is expected from more moisture in the atmosphere. However, cloud analysis

316 based on ERA5 reanalysis doesn't suggest significant effects of clouds. Total cloud
 317 cover in this region generally is larger than 90% in May and interannual anomaly is
 318 relatively small (less than 5%, see Fig. S5). This indicates that from the perspective of
 319 anomaly, water vapor rather than cloud cover has considerable radiation effects in the
 320 springtime. Given the large uncertainty of clouds in current datasets, this remains an
 321 open question.

322 ~~Other relevant variables can be found in Fig. S9.~~



326 **Fig. 5.** Scatter plots for 1979-2018 between the MA anomaly and region-mean
 327 anomalies of factors shown in Figs. 3 and 4. Thick dashed red lines denote linear fits
 328 above the 95% confidence level. **Below titles represent correlation above the 95%**
 329 **confidence level.**

330

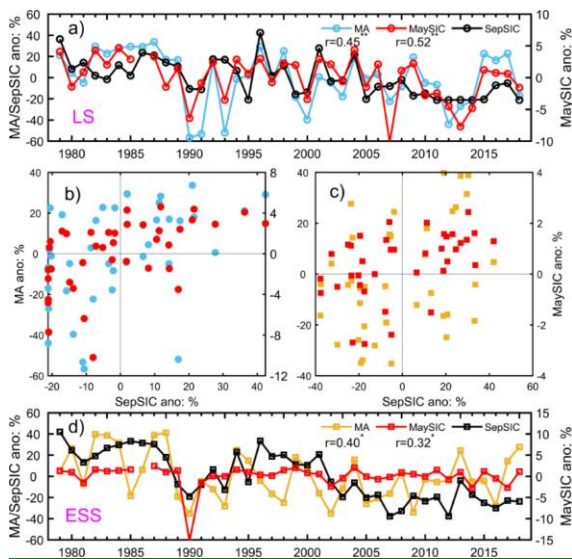
331 To what extent do different sea-ice surface melting scenarios in spring have
 332 implications for sea ice cover in summer? Could we gain seasonal prediction skill based
 333 on detection of sea-ice surface melting in spring? A simple way to address this is to put

Formatted: Normal (Web)

Field Code Changed

334 aside the processes linking spring and summer and directly investigate the statistical
335 relationship between sea-ice surface melting scenarios in spring and sea ice states in
336 summer. Figure 6 shows that in both the LS and ESS, Melt Advance in spring is
337 significantly correlated with sea ice cover in September, which is consistent with
338 previous studies utilizing Melt Onset as a predictor of summer sea ice (Petty et al., 2017;
339 Wang et al., 2011). However, it has no stronger prediction skill than SIC in May. In the
340 ESS, it seems that MA performs slightly better than May SIC predicting the September
341 SIC. The main reason may be that May SIC in the ESS has small interannual variability,
342 which is consistent with the lack of polynya activity in the ESS relative to the LS.
343 Beyond this, for the prediction of summer sea ice cover, the seasonal evolution from
344 spring to summer is still a challenge as it is not fully understood. Processes during the
345 melting season may strongly disturb the signal from the Melt Advance (Fig. S10). More
346 study of seasonal evolution in the Arctic is needed in the future.

347



348

349 Fig. 6. Sea-ice surface Melt Advance, SIC in May and September sea ice cover in the
350 Laptev Sea (subplot a and b) and East Siberian Sea (subplot c and d), 1979-2018.
351 September sea ice cover is denoted by the areal percentage of sea ice cover relative to
352 the whole sea. To facilitate viewing, Melt Advance is timed by -1. Correlation

353 coefficients with double asterisks denote 99% confidence, while those with a single
354 asterisk denote 90% confidence.

355

356

357 **4. Discussion**

358 In this study, sampling for different scenarios of sea ice Melt Advance is based on
359 the Melt Onset dataset, which is a satellite observation product. To our knowledge,
360 ERA5 to some extent incorporates the sea ice concentration dataset of OSI SAF, but
361 not the Melt Onset dataset (Hersbach et al., 2020). ERA5 atmospheric reanalysis and
362 different Melt Advance patterns can be seen as independent sources of information and
363 their consistency should provide more confidence.

364 In fact, the concept of Melt Advance can be used for the whole Arctic, and can
365 describe how sea-ice surface melting advances in spring. As mentioned above, Melt
366 Advance can also be used as relatively independent information with reference to an
367 atmospheric reanalysis dataset. Liang and Zhou (2023)~~In previous work, identified~~
368 ~~three modes of Melt Onset in the LS and ESS are identified~~ by EOF decomposition.
369 The positive L-mode and E-mode in their study correspond to LS-faster-scenario and
370 ESS-faster-scenario, while the positive and negative LE-mode relate to fast-scenario
371 and slow-scenario, respectively. (Liang and Zhou, 2023) (Liang and Zhou, 2023, in
372 press), and to some extent correspond to the different Melt Advance scenarios in this
373 work.

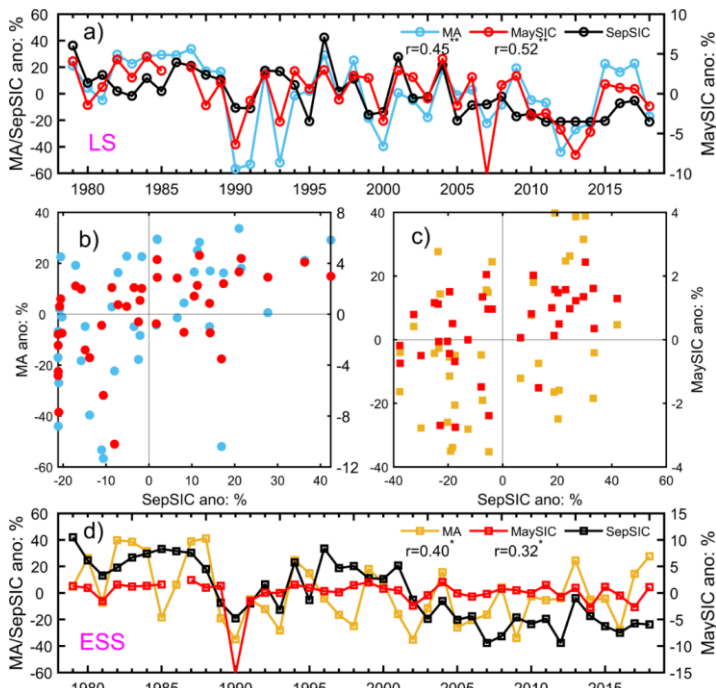
374 Regarding SIC anomaly in the LS and ESS, we should bear in mind that before
375 melting the shelf areas of the LS and ESS are covered with extensive fast ice (up to 200
376 km wide), which is formed by April (Selyuzhenok et al., 2015). SIC in May can increase
377 due to specific wind fields, but it probably does not consolidate against the land. Instead,
378 the SIC anomaly is closely related to polynya development. As Fig. 3 shows, the largest
379 SIC anomaly under the four scenarios usually occurs around the polynya region
380 (Willmes et al., 2011).

381 ~~To what extent do different sea ice surface melting scenarios in spring have~~

Field Code Changed

382 implications for sea ice cover in summer? Could we gain seasonal prediction skill based
383 on detection of sea ice surface melting in spring? A simple way to address this is to put
384 aside the processes linking spring and summer and directly investigate the statistical
385 relationship between sea ice surface melting scenarios in spring and sea ice states in
386 summer. Figure 6 shows that in both the LS and ESS, Melt Advance in spring is
387 significantly correlated with sea ice cover in September, which is consistent with
388 previous studies utilizing Melt Onset as a predictor of summer sea ice (Petty et al., 2017;
389 Wang et al., 2011). However, it has no stronger prediction skill than SIC in May.
390 Beyond this, for the prediction of summer sea ice cover, the seasonal evolution from
391 spring to summer is still a challenge as it is not fully understood. Processes during the
392 melting season may strongly disturb the signal from the Melt Advance (Fig. S10). More
393 study of seasonal evolution in the Arctic is needed in the future.

394



395
396 Fig. 6. Sea ice surface Melt Advance, SIC in May and September sea ice cover in the
397 Laptev Sea (subplot a and b) and East Siberian Sea (subplot c and d), 1979-2018.

398 ~~September sea ice cover is denoted by the areal percentage of sea ice cover relative to~~
399 ~~the whole sea. To facilitate viewing, Melt Advance is timed by 1. Correlation~~
400 ~~coefficients with double asterisks denote 99% confidence, while those with a single~~
401 ~~asterisk denote 90% confidence.~~

402

403

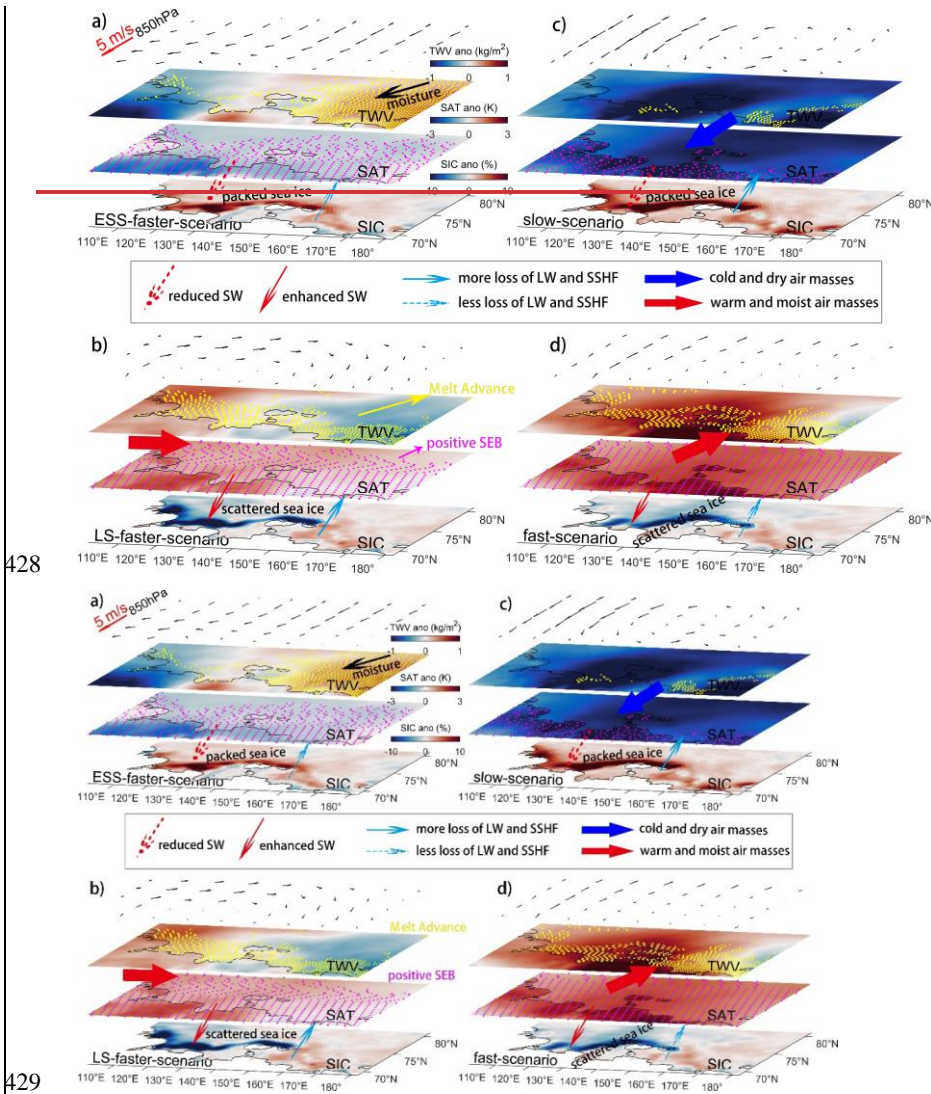
404 5. Conclusions

405 In this study, the metric of Melt Advance (MA) is used to measure sea-ice surface
406 melting instead of region-mean Melt Onset. MA is defined as the areal percentage of a
407 sea in which the sea ice surface has begun to melt at the end of May, in this case the
408 Laptev Sea (LS) and East Siberian Sea (ESS). This metric has the potential to help
409 seasonally predict summer sea ice, ~~as this can be a temporally changing variable. Melt~~
410 ~~Advance is also a potential metric~~ for the whole Arctic.

411 Four representative scenarios of Melt Advance in the LS and ESS are identified: the
412 ESS-faster-scenario, LS-faster-scenario, slow-scenario, and fast-scenario. Composite
413 analyses reveal that ~~in these distinct scenarios of Melt Advance, atmospheric circulation,~~
414 ~~sea ice dynamics (polynya activities), air mass advection, and surface energy fluxes are~~
415 ~~related with each other. the dominant driver is circulation in the lower troposphere,~~
416 ~~which regulates sea ice dynamics as well as air mass advection. The surface energy~~
417 ~~balance and sea ice Melt Advance are then influenced.~~ ESS-faster-scenario is
418 associated with positive TWV anomaly over the ESS and negative TWV anomaly over
419 the LS. LS-faster-scenario and fast-scenario seem to occur when polynya in the Laptev
420 Sea opens. But the slow-scenario mainly reflect the cool Arctic state in the 1980s. In
421 addition, polynya activity in this region and initial sea ice condition are also not
422 neglectable. The main conclusions are demonstrated in the schematic ~~in~~ of Fig. 7.

423 Although sea ice Melt Advance as well as sea ice cover in May are both statistically
424 correlated with sea ice cover in September, seasonal evolution can to a large extent
425 disturb this linkage. This study suggests a need to further investigate the changeable
426 spring circulation in the lower troposphere and seasonal evolution in the Arctic.

427



428

429

430 **Fig. 7.** Schematic processes under the four scenarios of sea ice Melt Advance in the LS
 431 and ESS. a) ESS-faster-scenario; b) LS-faster-scenario; c) slow-scenario; d) fast-
 432 scenario. For each scenario, four layers represent composite anomalies of wind fields
 433 at 850 hPa, TWV, SAT, and SIC, respectively. Thin arrows denote shortwave radiation
 434 (red), and longwave radiation and sensible heat flux (cyan), while solid and dashed
 435 types suggest the fluxes enhanced or weakened. Bold blue arrow refers to transport of
 436 cold and dry air masses, while bold red arrow refers to warm and moist advection.
 437 Yellow dots superimposed upon TWV show Melt Advance by the end of May. Magenta
 438 dots upon SAT denote positive surface energy balance (SEB).

Formatted: Normal (Web), Line spacing: single

439
440

Formatted: Justified, Line spacing: single

441 *Data Availability Statement.*

442 The sea ice MO dataset is from NASA's Cryospheric Sciences Research Portal
443 (<https://earth.gsfc.nasa.gov/cryo/data/arctic-sea-ice-melt>). SAT of IABP/POLES can be
444 accessed at <https://arcticdata.io/catalog/view/doi:10.18739/A2J598>, and SAT of AIRS
445 at https://disc.gsfc.nasa.gov/datasets/AIRS3STD_006/summary. The SIC dataset of
446 OSI SAF was downloaded from the websites below:
447 <ftp://osisaf.met.no/reprocessed/ice/conc/v2p0/> and
448 <ftp://osisaf.met.no/reprocessed/ice/conc-cont-reproc/v2p0/>.

449 The ERA5 reanalysis dataset was retrieved at
450 [https://cds.climate.copernicus.eu/cdsapp#!/search?type=dataset&keywords=\(\(%20%202Product%20type:%20Reanalysis%22%20\)\)](https://cds.climate.copernicus.eu/cdsapp#!/search?type=dataset&keywords=((%20%202Product%20type:%20Reanalysis%22%20))). In this study, we used ERA5 monthly
451 averaged data at single levels and pressure levels.
452

453

454 *Author Contribution*

455 Hongjie Liang [Formal analysis; Writing original draft].

456 Wen Zhou [Funding acquisition; Supervision].

457

458 *Competing interests*

459 The authors declare that they have no conflict of interest.

460

461 *Acknowledgments.*

462 This work was supported by the National Natural Science Foundation of China (Grant
463 No. 42288101, 42120104001).

464

465

466 REFERENCES

467 Bliss, A. and Anderson, M.: Snowmelt onset over Arctic sea ice from passive
468 microwave satellite data: 1979–2012, *The Cryosphere*, 8, 2089–2100, 10.5194/tc-
469 8-2089-2014, 2014.

470 Budyko, M. I.: The effect of solar radiation variations on the climate of the Earth, *Tellus*,
471 21, 611–619, 10.1111/j.2153-3490.1969.tb00466.x, 1969.

472 Cavalieri, D., Parkinson, C., Gloersen, P., and Zwally, H.: Sea ice concentrations from
473 Nimbus-7 SMMR and DMSP SSM/I passive microwave data, National Snow and
474 Ice Data Center, Boulder, Colorado, USA, 10.5067/8GQ8LZQVL0VL, 1996.

475 Cohen, J., Screen, J. A., Furtado, J. C., Barlow, M., Whittleston, D., Coumou, D.,

Formatted: Line spacing: single

Formatted: Justified

Formatted: Justified, Indent: Left: 0 cm,
Hanging: 2 ch, First line: -2 ch

- 476 Francis, J., Dethloff, K., Entekhabi, D., Overland, J., and Jones, J.: Recent Arctic
477 amplification and extreme mid-latitude weather, *Nature Geoscience*, 7, 627-637,
478 10.1038/ngeo2234, 2014.
- 479 Crawford, A. D., Horvath, S., Stroeve, J., Balaji, R., and Serreze, M. C.: Modulation of
480 Sea Ice Melt Onset and Retreat in the Laptev Sea by the Timing of Snow Retreat
481 in the West Siberian Plain, *Journal of Geophysical Research: Atmospheres*, 123,
482 8691-8707, 10.1029/2018jd028697, 2018.
- 483 Drobot, S. D. and Anderson, M. R.: An improved method for determining snowmelt
484 onset dates over Arctic sea ice using scanning multichannel microwave radiometer
485 and Special Sensor Microwave/Imager data, *Journal of Geophysical Research:*
486 *Atmospheres*, 106, 24033-24049, 10.1029/2000JD000171, 2001.
- 487 Francis, J. A. and Vavrus, S. J.: Evidence for a wavier jet stream in response to rapid
488 Arctic warming, *Environmental Research Letters*, 10, 10.1088/1748-
489 9326/10/1/014005, 2015.
- 490 Hersbach, H., Bell, B., Berrisford, P., Hirahara, S., Horányi, A., Muñoz - Sabater, J.,
491 Nicolas, J., Peubey, C., Radu, R., Schepers, D., Simmons, A., Soci, C., Abdalla,
492 S., Abellan, X., Balsamo, G., Bechtold, P., Biavati, G., Bidlot, J., Bonavita, M.,
493 Chiara, G., Dahlgren, P., Dee, D., Diamantakis, M., Dragani, R., Flemming, J.,
494 Forbes, R., Fuentes, M., Geer, A., Haimberger, L., Healy, S., Hogan, R. J., Hólm,
495 E., Janisková, M., Keeley, S., Laloyaux, P., Lopez, P., Lupu, C., Radnoti, G.,
496 Rosnay, P., Rozum, I., Vamborg, F., Villaume, S., and Thépaut, J. N.: The ERA5
497 global reanalysis, *Quarterly Journal of the Royal Meteorological Society*, 146,
498 1999-2049, 10.1002/qj.3803, 2020.
- 499 Horvath, S., Stroeve, J., Rajagopalan, B., and Jahn, A.: Arctic sea ice melt onset favored
500 by an atmospheric pressure pattern reminiscent of the North American-Eurasian
501 Arctic pattern, *Climate Dynamics*, 57, 1771-1787, 10.1007/s00382-021-05776-y,
502 2021.
- 503 Kashiwase, H., Ohshima, K. I., Nihashi, S., and Eicken, H.: Evidence for ice-ocean
504 albedo feedback in the Arctic Ocean shifting to a seasonal ice zone, *Sci Rep*, 7,
505 8170, 10.1038/s41598-017-08467-z, 2017.
- 506 Krumpfen, T., Hölemann, J. A., Willmes, S., Morales Maqueda, M. A., Busche, T.,
507 Dmitrenko, I. A., Gerdes, R., Haas, C., Heinemann, G., Hendricks, S., Kassens,
508 H., Rabenstein, L., and Schröder, D.: Sea ice production and water mass
509 modification in the eastern Laptev Sea, *Journal of Geophysical Research*, 116,
510 10.1029/2010jc006545, 2011.
- 511 Lavergne, T., Sørensen, A. M., Kern, S., Tonboe, R., Notz, D., Aaboe, S., Bell, L.,
512 Dybkjær, G., Eastwood, S., Gabarro, C., Heygster, G., Killie, M. A., Brandt
513 Kreiner, M., Lavelle, J., Saldo, R., Sandven, S., and Pedersen, L. T.: Version 2 of
514 the EUMETSAT OSI SAF and ESA CCI sea-ice concentration climate data
515 records, *The Cryosphere*, 13, 49-78, 10.5194/tc-13-49-2019, 2019.
- 516 Lei, R., Cheng, B., Hoppmann, M., Zhang, F., Zuo, G., Hutchings, J. K., Lin, L., Lan,
517 M., Wang, H., Regnery, J., Krumpfen, T., Haapala, J., Rabe, B., Perovich, D. K.,

518 and Nicolaus, M.: Seasonality and timing of sea ice mass balance and heat fluxes
519 in the Arctic transpolar drift during 2019–2020, *Elementa: Science of the*
520 *Anthropocene*, 10, 10.1525/elementa.2021.000089, 2022.

521 Liang, H. and Su, J.: Variability in Sea Ice Melt Onset in the Arctic Northeast Passage:
522 Seesaw of the Laptev Sea and the East Siberian Sea, *Journal of Geophysical*
523 *Research: Oceans*, 126, e2020JC016985, 10.1029/2020JC016985, 2021.

524 Liang, H. and Zhou, W.: Arctic Sea Ice Melt Onset in the Laptev Sea and East Siberian
525 Sea in Association with the Arctic Oscillation and Barents Oscillation, *Journal of*
526 *Climate*, 36, 6363–6373, 10.1175/jcli-d-22-0791.1, 2023.

527 Markus, T., Stroeve, J. C., and Miller, J.: Recent changes in Arctic sea ice melt onset,
528 freezeup, and melt season length, *Journal of Geophysical Research (Oceans)*, 114,
529 C12024, 10.1029/2009jc005436, 2009.

530 Mortin, J., Svensson, G., Graverson, R. G., Kapsch, M.-L., Stroeve, J. C., and Boisvert,
531 L. N.: Melt onset over Arctic sea ice controlled by atmospheric moisture transport,
532 *Geophysical Research Letters*, 43, 6636–6642, 10.1002/2016GL069330, 2016.

533 Petty, A. A., Kurtz, N. T., Kwok, R., Markus, T., and Neumann, T. A.: Winter Arctic Sea
534 Ice Thickness From ICESat - 2 Freeboards, *Journal of Geophysical Research:*
535 *Oceans*, 125, 10.1029/2019jc015764, 2020.

536 Petty, A. A., Schröder, D., Stroeve, J. C., Markus, T., Miller, J., Kurtz, N. T., Feltham,
537 D. L., and Flocco, D.: Skillful spring forecasts of September Arctic sea ice extent
538 using passive microwave sea ice observations, *Earth's Future*, 5, 254–263,
539 10.1002/2016ef000495, 2017.

540 Screen, J. A. and Simmonds, I.: The central role of diminishing sea ice in recent Arctic
541 temperature amplification, *Nature*, 464, 1334–1337, 10.1038/nature09051, 2010.

542 Sellers, W. D.: A Global Climatic Model Based on the Energy Balance of the Earth-
543 Atmosphere System, *Journal of Applied Meteorology and Climatology*, 8, 392-
544 400, 10.1175/1520-0450(1969)008<0392:agcmbo>2.0.co;2, 1969.

545 Selyuzhenok, V., Krumpen, T., Mahoney, A., Janout, M., and Gerdes, R.: Seasonal and
546 interannual variability of fast ice extent in the southeastern Laptev Sea between
547 1999 and 2013, *Journal of Geophysical Research: Oceans*, 120, 7791–7806,
548 10.1002/2015jc011135, 2015.

549 Serreze, M. C., Barrett, A. P., Stroeve, J. C., Kindig, D. N., and Holland, M. M.: The
550 emergence of surface-based Arctic amplification, *The Cryosphere*, 3, 11–19,
551 10.5194/tc-3-11-2009, 2009.

552 Skeie, P.: Meridional flow variability over the Nordic Seas in the Arctic oscillation
553 framework, *Geophysical Research Letters*, 27, 2569–2572, 10.1029/2000gl011529,
554 2000.

555 Stroeve, J. and Notz, D.: Changing state of Arctic sea ice across all seasons,
556 *Environmental Research Letters*, 13, 103001, 10.1088/1748-9326/aade56, 2018.

557 Stroeve, J. C., Markus, T., Boisvert, L., Miller, J., and Barrett, A.: Changes in Arctic
558 melt season and implications for sea ice loss, *Geophysical Research Letters*, 41,
559 1216–1225, 10.1002/2013gl058951, 2014.

- 560 Taylor, P. C., Boeke, R. C., Boisvert, L. N., Feldl, N., Henry, M., Huang, Y., Langen, P.
561 L., Liu, W., Pithan, F., Sejas, S. A., and Tan, I.: Process Drivers, Inter-Model
562 Spread, and the Path Forward: A Review of Amplified Arctic Warming, *Frontiers*
563 *in Earth Science*, 9, 10.3389/feart.2021.758361, 2022.
- 564 Wang, L., Wolken, G. J., Sharp, M. J., Howell, S. E. L., Derksen, C., Brown, R. D.,
565 Markus, T., and Cole, J.: Integrated pan-Arctic melt onset detection from satellite
566 active and passive microwave measurements, 2000-2009, *Journal of Geophysical*
567 *Research: Atmospheres*, 116, 10.1029/2011jd016256, 2011.
- 568 Willmes, S., Adams, S., Schröder, D., and Heinemann, G.: Spatio-temporal variability
569 of polynya dynamics and ice production in the Laptev Sea between the winters of
570 1979/80 and 2007/08, *Polar Research*, 30, 10.3402/polar.v30i0.5971, 2011.

571